IR LASER CVD OF NANODISPERSE Ge-Si-Sn ALLOYS OBTAINED BY DIELECTRIC BREAKDOWN OF $GeH_4/SiH_4/SnH_4$ MIXTURES

Tomáš KŘENEK*[a,b], Petr BEZDIČKA[c] Nataliya MURAFA,[c] Jan ŠUBRT[c],and Josef POLA[a]

[a]*University of West Bohemia, Research Centre New Technologies 30614 Plzen, Czech Republic*
[b]*Department of Aerosols and Laser Studies, Institute of Chemical Process Fundamentals, Academy of Sciences of the Czech Republic, 16502 Prague, Czech Republic*
[c]*Institute of Inorganic Chemistry, Academy of Sciences of the Czech Republic, 25068 Řež, Czech Republic*
**tkrenek@ntc.zcu.cz*

Abstract

Nowadays, great attention is devoted to Ge-Si-Sn ternary system, because $Si_{1-x-y}Ge_xSn_y$ provides the potential of band gap engineering and tuning of the optical properties. IR laser irradiation of equimolar gaseous GeH_4 + SiH_4 + SnH_4 + Ar mixture results in simultaneous decomposition of all three compounds and it allows deposition of nanostructured solid film. Analysis of the films by FTIR and Raman spectroscopy, X-ray diffraction analysis and electron microscopy revealed crystalline nanobodies of pure β-Sn and crystalline nanoobjects of $Ge_{1-x-y}Si_xSn_y$ embedded in an amorphous metastable Ge-Si-Sn alloy. This process allows co-decomposition of all silicon, germanium and tin hydrides which is caused by combination of infrared multiple photon dissociation of absorbing silane and currently proceeding LIDB. This is followed by intermixing/clustering of extruded metal atoms in the gas phase.

Keywords: IR laser, Thermal decomposition, Ge/Si/Sn nanoalloys, Metastable compounds

1. INTRODUCTION

Research of ternary Si-Ge-Sn preceded investigation of Sn_xGe_{1-x} alloys (analogous to the well-known $Si_{1-x}Ge_x$) with non-equilibrium composition of both elements (higher Ge content in the solid phase), because these alloys posses a great potential of a tunable direct energy gap[1]. It has been also found that $Ge_{1-y}Sn_y$ layers have ideal properties as templates for the subsequent deposition of other semiconductors[2]. The formation of *bulk* Sn_xGe_{1-x} alloys[3] with the solid solubility limit of Ge in Sn diamond-cubic structure > 1% is difficult due to (i) large lattice mismatch (15 %) between Ge and α-Sn and (ii) instability of d-c α-Sn phase at ambient temperature. Such alloys can be fabricated only as metastable nano-sized films by using special techniques allowing a non-equilibrium growth[eg. 4, 5].
Nowadays, great attention is devoted to Ge-Si-Sn ternary system, because $Si_{1-x-y}GexSny$ provides the potential of band gap engineering and tuning of the optical properties[6]. Si–Ge–Sn materials represent the first practical group IV ternary alloy, because C can only be incorporated in minute amounts to the Ge-Si network[7].
The most significant feature of $Si_{1-x-y}Ge_xSn_y$ system is the possibility of independent adjustment of the lattice constant and band gap[8]. A linear interpolation of band gap lattice constants between Si, Ge, and α-Sn shows that it is possible to obtain SiGeSn with a band gap and a lattice constant larger than that of Ge [2]. For the same value of the lattice constant can be obtained band gap differing by >0.2 eV, even if the Sn concentration is limited to the range y < 0.2[2]. Incorporation of Si into Sn_yGe_{1-y} leads to an additional reduction of the critical point that is based on the critical point values of Si and Ge[9].
These properties make Ge-Si-Sn alloy a promising candidate for developing of a various novel devices span from multicolor detectors (SiGeSn alloy provides a novel approach to extend the utility of pure Ge in IR emission), sensing technologies, semiconductor lasers, high-speed modulators, to multiple-junction photovoltaic cells[2]. A tensile-strain-induced direct gap of Ge can be used also for laser diodes and electroptical modulators[2]. SiGeSn systems enable buffer layer technologies with unprecedented lattice and

thermal matching capabilities for applications in monolithic integration of III - V semiconductors with Si electronics[7].

There have been proposed a strain-free Ge/$Ge_{0.76}$ $Si_{0.19}Sn_{0.05}$ quantum cascade laser using intersubband transitions at *L* valleys of the conduction band which has a "clean" offset of 150 meV situated below other energy valleys [10]. Longer lifetimes due to the weaker scattering of nonpolar optical phonons reduce the threshold current and potentially lead to room temperature operation[10].

Till now, UHVCVD reactions of the gaseous compound SiH_3GeH_3 with SnD4 at 350 °C allowed formation of single-phase $Si_{1-x-y}Ge_xSn_y$ alloys with random diamond cubic structures deposited on Si(100) substrate[8]. Here, commensurate heteroepitaxy was facilitated by $Ge_{1-x}Sn_x$ buffer layers, which acted as templates that could conform structurally and absorb the differential strain imposed by the more rigid Si and Si–Ge–Sn materials[8]. In this work[8] was demonstrated growth of perfectly epitaxial, uniform and highly aligned layers with atomically smooth surfaces and monocrystalline structures that have lattice constants close to that of Ge. In this case compositions of films grown on $Ge_{1-x}Sn_x$ span form $Si_{0.14}Ge_{0.84}Sn_{0.02}$ to $Si_{0.14}Ge_{0.80}$ $Sn_{0.06}$. Single-phase monocrystalline $Ge_{1-x-y}Si_xSn_y$ alloys that possess a variable and controllable range of compositions and exhibit lattice constants above and below that of bulk Ge have been grown on Si(100) via $Ge_{1-y}Sn_y$ buffers[9]. The growth of $Ge_{1-x-y}Si_xSn_y$ has been accomplished by using the SiH_3GeH_3, $(GeH_3)_2SiH_2$, and $(GeH_3)_3SiH$ hydrides as the source of the Si and Ge atoms. These were the key precursors that furnish the building blocks of specifically tailored elemental contents and possess the necessary reactivity to readily form the desired metastable structures and concentrations at low temperatures of 300–350 °C.

An attention has been devoted also to an empirical model providing a quantitative description of the composition dependence of the lattice[9]. First principles simulations predict that these materials are thermodynamically accessible and yield lattice constants as a function of Si/Sn concentrations in good agreement with experiment[9]. There have been found that ternary SiSnGe alloys form more readily, and exhibit greater thermal stability than their SnGe counterpart[9]. This could be caused by the strain equalization which results from opposing effect of the Si and Sn incorporation. It has been indicated that low % Sn alloys are thermodynamically stable while the 7-8 % Sn alloys are only slightly metastable [9]. Theoretical model for optical gain of a strained $Sn_{1-x-y}Si_xGe_y$ quantum well (QW) structure has been described in literature[11].

Here, we have been proposed the method for the creation of ternary nanoalloy via IR laser induced gas-phase co-decomposition of three mixed compounds which allows formation of nanoalloy particles in the gas phase through interaction between simultaneously generated (different) atoms and their clusters.

We report on IR LCVD of Ge/Si/Sn ternary metastable alloy through co-decomposition of SiH_4, GeH_4 and SnH_4 in IR LIDB (where also infrared multiple photon decomposition of absorbing silane[20, 21] proceeds). This process leads to the deposition of nanostructured film consisted of Ge-Si-Sn nanoparticles and pure crystalline β-Sn nanoparticles which are surrounded by an amorphous alloy matrix.

The presented results follow our previous research on LI CVD of SnGe[12,13], SnSi[14], SiGe[15] nanostructured alloys.

2. EXPERIMENTAL

The laser-irradiation of GeH_4-SnH_4–SiH_4 (total pressure of precursors 10 Torr, ratio 1:1:1) in Ar (total pressure 110 Torr) was accomplished with a TEA CO2 laser (Plovdiv University, model 1300M) operating with a repetition frequency of 1 Hz at the P(20) line of the $00^01 \rightarrow 10^00$ transition (944.19 cm^{-1}) and pulse energy 1.8 J. The gaseous mixture was irradiated in a Pyrex reactor fitted with KBr windows and PTFE valve connecting to vacuum manifold and pressure transducer. The laser pulse was focused with a NaCl lens (f.l. 15 cm) to the centre of the reactor[12], above which was accommodated a silicon substrate. The mixture was irradiated by 45 pulses and the thin films on the Si substrate were deposited through 3 cycles. The progress of the co-decomposition of SnH_4 and SiH_4 and GeH_4 was monitored by FTIR spectroscopy (a Nicolet Impact spectrometer) using absorption bands at 677 and 1902 cm^{-1} (SnH_4) and 908 and 2186 cm^{-1}

(SiH_4) and 816 cm^{-1} and 2108 cm^{-1} (GeH_4). Thereafter, the reactor was evacuated and the Si substrate was ransferred in a sealed vial under Ar (to prevent its oxidation) for spectral and electron microscopy analyses. FTIR reflection spectra were recorded on a Nicolet Impact spectrometer (resolution 4 cm^{-1}) and Raman spectra were obtained using a dispersive Raman instrument Nicolet Almega XR (resolution 2 cm^{-1}), excitation wavelength 473 nm and power 10 mW). SEM analyses were carried out on a Philips XL30 CP scanning electron microscope and energy dispersive X-ray (EDX) analyses were conducted on a Philips XL30 CP instrument equipped with an EDX detector PV 9760 using accelerating voltage 5–30 kV. Transmission electron microscopy (TEM) and high-resolution transmission electron microscopy (HRTEM) micrographs were carried out on a JEOL JEM 3010 microscope operated at 300 kV (LaB6 cathode, point resolution 1.7 Å) with an energy dispersive Xray (EDX) detector attached. Copper grid coated with a holey carbon film was used to samples prepare. A fine powder of deposit was transferred onto a grid and used for the TEM observation. Diffraction patterns were collected with a PANalytical X'Pert PRO diffractometer equipped with a conventional X-ray tube (Co Ka radiation, 40 kV, 30 mA, point focus), an X-ray monocapillary with diameter of 0.1 mm, and a multichannel detector X'Celerator with an anti-scatter shield through a procedure reported previously[12]. XRD patterns were not pre-treated before interpretation, as no background correction was needed. Qualitative analysis was performed with HighScore software package (PANalytical, The Netherlands, Version 1.0d), Diffrac-Plus software package (Bruker AXS, Germany, Version 8.0) and JCPDS PDF-2 database[16]. For quantitative analysis of XRD patterns we used Diffrac-Plus Topas (Bruker AXS, Germany, Version 4.1) with structural models based on ICSD database[17]. This program permits to determine the unit cell parameters and to estimate the weight fractions of crystalline phases and also to estimate the amorphous content (the ''degree of crystallinity'') by means of Rietveld refinement procedure.
Stannane (prepared by treating tin tetrachloride with lithium aluminium hydride[18]) and germane obtained by reaction between germanium dioxide and potassium tetrahydroborate[19] and silane (Lachema, >99.5% pure) were distilled on vacuum line and checked for purity by FTIR spectroscopy.

3. RESULTS AND DISCUSION

The SiH_4 has absorption band coinciding with P(20) line of the $00^01 \rightarrow 10^00$ transition (944.19 cm^{-1}) of CO_2 laser. The GeH_4 and SnH_4 do not have absorption band centered at this laser line but the highly focused radiation induces interaction leading to dielectric breakdown (a visible spark) and results in a decomposition of all GeH_4 and SiH_4 and SnH_4 yielding elemental metals in the gas phase and allowing deposition of ultrafine solid on the Si substrate. The decomposition of the silane is caused probably by both the infrared multiple photon decomposition[20, 21] and the collisionally assisted decomposition of silane[22] and the depletion of non-absorbing germane and stannane by collisionally assisted decomposition[22]. The absorption bands of the Si, Ge and Sn progenitors diminishing at a similar rate and respectively depleting by 35 and 45 % with 50 pulses indicate similar consumption of Si, Ge and Sn for the formation of the solid deposit.
FTIR spectroscopy of the deposited film does not reveal any evidence of Si-H, Ge-H and Sn-H bonds (respectively located at ~1890, 2000 cm^{-1} and 1900 cm^{-1}) typical for a-Sn_xGe_{1-x}:H structures (e.g. [23]) or for a-Si_xGe_{1-x}:H structures[24] and confirms a complete elimination of H from all progenitors.
SEM images of the deposit (Fig. 1) reveal fluffy morphology with less than μm-sized bodies merging into several μm large agglomerates. The EDX analyses indicate small contamination by O and C elements and reveal stoichiometries $Sn_1Ge_{0.95}Si_{10.60}$ for 300 μm^2 area and $Sn_1Ge_{0.78}Si_{1.27}$ for several μm-sized particles that agree with the relative decomposition of the metal hydrides. From SEM images (Fig. 1) from EDX of 300 μm^2 area follows that Sn-Ge-Si particles do not cover the Si substrate completely.

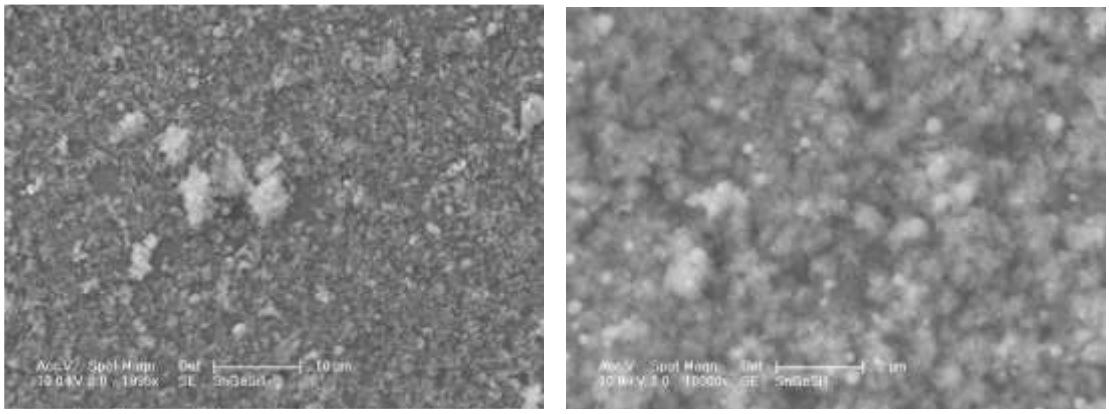

Fig. 1 Typical SEM images of the deposit.

Raman spectra of the deposited film (Fig. 2) shows the broad peak positioned at 265 – 283 cm^{-1} is assigned in its extreme value (265 cm^{-1}) to $Ge_{1-y}Sn_y$ alloy with y = 0.02[eg. 8]. The other extreme of this peaks (283 cm^{-1}) is assigned to Ge-Ge* bond in $Ge_{1-y}Sn_y$ alloy with y = 0.25[eg. 8]. However, it is probable that this peak includes also some amount of Si atoms. Ge and Si are miscible in all contents and thus very feasible for formation Ge-Si alloys[eg. 3]. From that it could be considered that this peaking represents Ge-Sn-Si alloy where we can assume opposite effect of Sn and Si incorporation on the position of Raman peak - i.e. the incorporation of Sn atoms into Ge lattice leads to an downshift[25] of the Raman value and that that of Si atoms into Ge lattice upshifts the Raman peak[eg. 8].
Peaking centered at 380 – 390 cm^{-1} agrees with Si-Ge vibration of $Si_{1-x}Ge_x$ alloy where x ~ 0.96 [25]. Here could be possible presence of substitutional Sn which *would* induce downshift of Raman peaks [25]. This aspect is caused by substitutional Sn-induced lattice expansion[25].
Broad band around 480 cm^{-1} is assigned to amorphous Si [175] and it could also demonstrate contribution of Si-Si* vibration corresponds to $Si_{1-x}Ge_x$ alloy with x = 0.6[25]. If we speculate again about presence of amount of substitutional Sn we have to consider certain downshift of Raman values. Sharp band positioned at 515-520 cm^{-1} coincides with Si-Si bond of Si substrate[eg. 25].

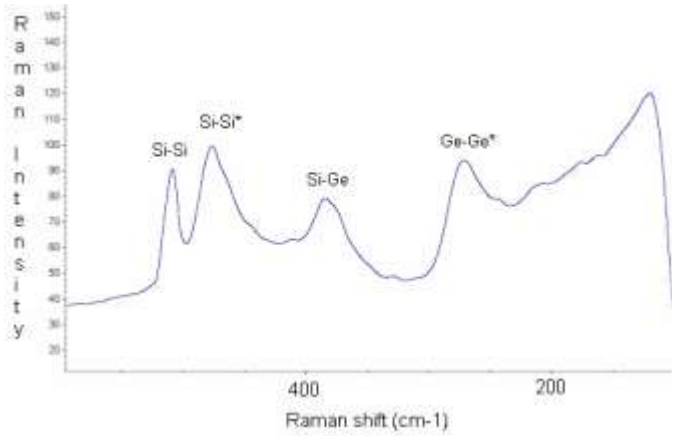

Fig. 2 Typical Raman spectrum of the Si-Ge-Sn deposit showing Si-Si, Si-Si*, Si-Ge and Ge-Ge* peaks.

The μ-XRD analysis (Fig. 3) reveals the presence of two crystalline phases, one with the unit cell parameters a = 0.5831 nm and c = 0.3182 nm which corresponds to tetragonal β-Sn (existing at temperatures >13.25 ^oC) and another with the unit cell parameter a = 0.5683 nm which could be assigned to Ge-Sn alloy. The unit cell parameter of pure d-c Ge is a = 0.5657 nm. This increasing of the cell parametr reflects, in agreement with literature[26], approximately 4 % incorporation of Sn atoms into Ge lattice. However, if we consider the

formation of Ge-Si-Sn ternary alloy we have to reflect on both increasing effect of substitutional Sn on Ge d-c lattice parameter[26] and decreasing influence of substitutional Si on Ge d-c lattice parameter[2].

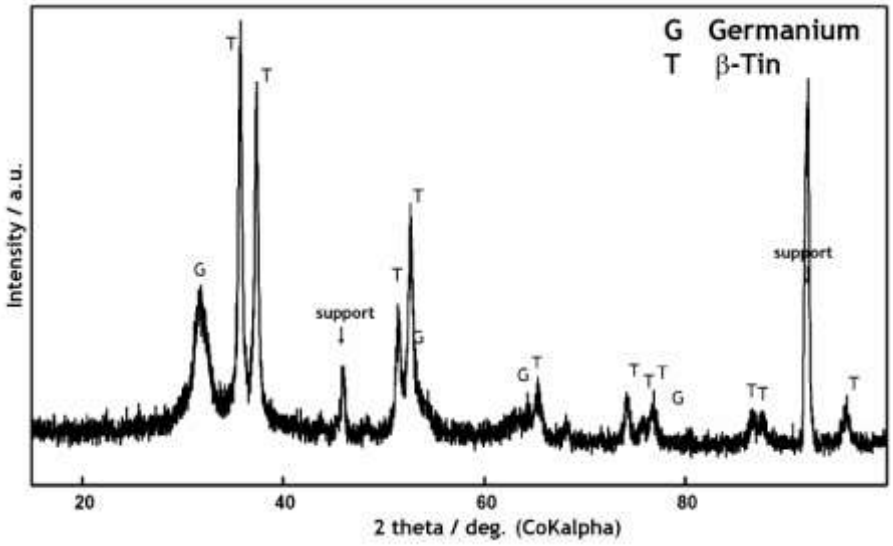

Fig. 3 μ-XRD analysis of the deposit.

The TEM image (Fig. 4a) reveals irregular agglomerates consisting of uniform amorphous plates with embedded spherical nanoparticles (10–50 nm). The EDX analysis of the deposit indicates great amount of Sn and Ge and Si and small contamination of C and O. The HRTEM micrographs (Fig. 4b,c) show nanostructures consisting of a blend of crystalline and amorphous phase where crystalline and amorphous phases mutually blend into one another without sharp borders. The examples of HRTEM images (Fig. 4b,c) reveal crystalline nanoparticles with interlayer spacing of d = 0.289 nm (Fig. 4b) and d = 0.290 nm (Fig. 4c), the values corresponding to the tetragonal Sn (PDF 04-0673) and correspond to the distance between (200) crystal planes.

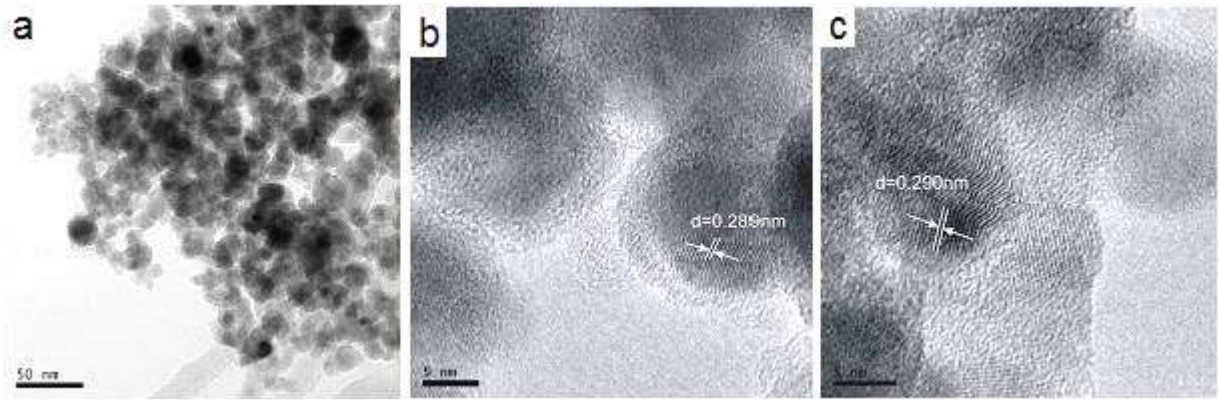

Fig. 4 TEM (a) and HRTEM (b and c) micrographs of the deposit.

4. CONCLUSION

IR laser irradiation of equimolar gaseous GeH4 + SiH4 + SnH4 + Ar mixture results in simultaneous decomposition of all three compounds and it allows deposition of nanostructured solid film consisting of crystalline nanobodies of pure β-Sn and crystalline nanoobjects of $Ge_{1-x-y}Si_xSn_y$ embedded in an amorphous metastable Ge-Si-Sn alloy.

This process allows co-decomposition of all silicon, germanium and tin hydrides which is caused by combination of infrared multiple photon dissociation of absorbing silane and currently proceeding LIDB. This is followed by intermixing/clustering of extruded metal atoms in the gas phase.

ACKNOWLEDGEMENTS

This research was carried out within the CENTEM project, reg.no. CZ.1.05/2.1.00/03.0088, co-funded by the ERDF as part of the Ministry of Education, Youth and Sports' OP RDI programme.

REFERENCES

[1] KOUVEKATIS, J., MAYER, J. W., Optoelectronic Properties of Semiconductors and SuperLattice, Vol.15. Silicon-Germanium Carbon Alloy, Edited by S.T. Pantelides and S. Zollner, Chapter 2 , 19-58, 2002, Taylor & Francis Books.

[2] SOREF, R., KOUVEKATIS, J., TOLLE, J., MENENDEZ, J., D'COSTA, V., *Journal of Materials Research*, Vol. 22, Issue: 12, 2007, 3281-3291.

[3] SGTE alloy phase diagrams databases, 2004.

[4] BENNET, J. C., EGERTON, R. F., *Vacuum*, *47*, 1996, 1419–1422.

[5] FUKUMOTO, H., MYOREN, H., NAKASHITA, T., IMURA, T., OSAKA, Y., *Jpn. J. Appl. Phys.*, *25*, 1986, 1312–1346.

[6] SOREF, R. A. and PERRY, C. H., *J. Appl. Phys.* 69, 1991, 539.

[7] KOUVEKATIS, J., CHIZMESHYA, A.V.G., ANDREW, V. G., *JOURNAL OF MATERIALS CHEMISTRY*, Vol. 17, Issue: 17, 2007, 1649-1655.

[8] BAUER, M., COLE, R., CROZIER, P. A. , REN, J., MENENDEZ, J., WOLF, G., KOUVEKATIS, J. S, *Appl. Phys. Lett*., Vol. 83, 2003, No. 11.

[9] AELLA, P., COOK, C., TOLLE, J., ZOLLNER, S., CHIZMESHYA, A.V.G., KOUVETAKIS, J., *APPLIED PHYSICS LETTERS*, Vol. 84, Issue: 6, 2004, 888-890.

[10] SUN, G., GHENG, H. H., *APPLIED PHYSICS LETTERS*, Vol. 90, Issue: 25, 2007, Article Number: 251105.

[11] CHANG, Shu-Wei, CHUANG, Shun Lien, *IEEE JOURNAL OF QUANTUM ELECTRONICS*, Vol. 43 Issue: 3-4, 2007, 249 -256.

[12] KŘENEK, T., BEZDIČKA, P., MURAFA, N., ŠUBRT, J., POLA, *J., Eur. J. Inorg. Chem.* , 2009, 1464–1467.

[13] KŘENEK, T., BEZDIČKA, P., MURAFA, N., ŠUBRT, J., POLA, *J., Appl. Organometal. Chem.* 24, 2010, 458–463.

[14] KŘENEK, T., BEZDIČKA, P., MURAFA, N., ŠUBRT, J., DUCHEK, P., POLA, J., *J. Anal. Appl. Pyrol*.86, 2009, 381–385.

[15] KŘENEK, T., BEZDIČKA, P., MURAFA, N., ŠUBRT, J., POLA, J., *Journal of Analytical and Applied Pyrolysis* 89, 2010, 137–141

[16] JCPDS PDF-2 database, International Centre for Diffraction Data, Newton Square, PA, USA release 54, 2004.

[17] ICSD database FIZ Karlsruhe, Germany, release 2008/1, 2008.

[18] REIFENBERG, G.H., CONSIDINE, W.J., *Organometallics* 12, 1993, 3015–3018.

[19] JOLLY, W. I., DRAKE, J. E., *Inorg. Synthesis* **1963**, *7*, 34–44.

[20] DEUTSCH, T.F., *J. Chem. Phys.* 70, **1979**, 1187-1192.

[21] LONGWAY, P.A., LAMPE, F.W., *J. Am. Chem. Soc.* 103, **1981**, 6813-6818.

[22] LAMPE, F.W., *Spectrochim. Acta A* 43, **1987,** 257-264.

[23] CHIN-PRADO E., KATIYAR, R.S., MUNOZ, W., ERSTO, O., WEISZ, S.Z., *Phys. Rev. B* **1994**, *50*, 11653-11660.

[24] CHO, S.M., CHRISTENSEN, C., LUCOVSKY, G., MAHER, D.M., *Journal of Non-Crystalline Solids,* 1996, 198-200, 587-591

[25] SHIN, H.K., *Solid State Communications* 114, 2000, 505–510

[26] BAUER, M.R., TOLLE, J., BUNGAY, C., CHIYMESHZA, A.V.G., SMITH, D.J., MENENDEZ, J., KOUVEKATIS, J., *Solid St. Commun*. **2003**, *127*, 355.